Differential Geometry and its Applications 27 (2009) 527–542

Contents lists available at ScienceDirect

Differential Geometry and its Applications

www.elsevier.com/locate/difgeo

Immersions of the projective plane with one triple point

Sue Goodman [a,*], Marek Kossowski [b]

[a] University of North Carolina, Chapel Hill, USA
[b] University of South Carolina, Columbia, USA

ARTICLE INFO

Article history:
Received 18 September 2007
Received in revised form 28 July 2008
Available online 5 February 2009
Communicated by J. Stasheff

MSC:
53A05
57R42
53C42

Keywords:
Immersion
Projective plane
Triple point
Isotropy

ABSTRACT

We consider C^∞ generic immersions of the projective plane into the 3-sphere. Pinkall has shown that every immersion of the projective plane is homotopic through immersions to Boy's immersion, or its mirror. There is another lesser-known immersion of the projective plane with self-intersection set equivalent to Boy's but whose image is not homeomorphic to Boy's. We show that any C^∞ generic immersion of the projective plane whose self-intersection set in the 3-sphere is connected and has a single triple point is ambiently isotopic to precisely one of these two models, or their mirrors. We further show that any generic immersion of the projective plane with one triple point can be obtained by a sequence of toral and spherical surgical modifications of these models. Finally we present some simple applications of the theorem regarding discrete ambient automorphism groups; image-homology of immersions with one triple point; and almost tight ambient isotopy classes.

In this paper we consider C^∞ generic immersions of the projective plane into the 3-sphere, $i:\mathbb{P}^2\to\mathbb{S}^3$. Pinkall [14] has shown that every immersion of the projective plane is isotopic to Boy's immersion i_{b^+}, or its mirror $i_{b^-}=R\circ i_{b^+}$ where R is a reflection. The image of $i_{b^\pm}$ intersects itself on a C^∞ immersed circle in $\mathbb{S}^3$. The image of this circle intersects itself at a unique triple point, creating a bouquet of three unlinked, unknotted loops in $\mathbb{S}^3$. There are three disks in $\mathbb{P}^2$ whose images under $i_{b^\pm}$ are embedded and whose boundaries are precisely these three loops. Apery [1] described an isotopy of Boy's immersion that produces an immersion $i_{g^+}:\mathbb{P}^2\to\mathbb{S}^3$ whose self-intersection set is equivalent to Boy's but one of the three loops does not bound such an image disk. Hence the preimages of the self-intersection curves for $i_{b^\pm}$ versus $i_{g^\pm}$ must be topologically distinct. This paper exploits this structural difference to prove: *If $i:\mathbb{P}^2\to\mathbb{S}^3$ is a C^∞ generic immersion whose self-intersection set in $\mathbb{S}^3$ is connected and has a single triple point then i is ambiently isotopic to $i_{b^\pm}$ or $i_{g^\pm}$* (Theorem 4.3). That is to say, if the self-intersection set is connected and has only one triple point then this set must be a bouquet of three unlinked, unknotted, C^0 closed curves, and the projective plane can be "sewn into" this set in essentially two distinct ways. Theorem 4.3 is a refinement of Apery's classification of immersions of $\mathbb{P}^2$ [2]. As an application we can present any generic immersion of $\mathbb{P}^2$ with one triple point as $i_{b^\pm}$ or $i_{g^\pm}$ modified by a sequence of toral and spherical surgeries (Theorem 5.2).

Recall that two immersions i_0, i_1 are ***equivalent*** ($i_0\equiv i_1$) if there exist C^∞ diffeomorphisms Φ of $\mathbb{S}^3$, and ϕ of $\mathbb{P}^2$ such that $i_1=\Phi\circ i_0\circ\phi$. They are ***isotopic*** if there exists a homotopy through C^∞ immersions i_t, $t\in[0,1]$, connecting the given immersions. They are ***ambiently isotopic*** if there exist homotopies ϕ_t,Φ_t, $t\in[0,1]$, $\Phi_0=id$, through C^∞ diffeomorphisms of $\mathbb{P}^2$ and $\mathbb{S}^3$ respectively such that $i_t=\Phi\circ i_0\circ\phi$ connects $i_0\equiv i_0\circ\phi_0$ and $i_1\equiv\Phi_1\circ i_1\circ\phi_1$. Note that the reference to ϕ_t

* Corresponding author.
E-mail address: seg@email.unc.edu (S. Goodman).

0926-2245/$ – see front matter
doi:10.1016/j.difgeo.2009.01.011

is usually omitted in the definition of ambient isotopy. However we will use the implicit intrinsic isotopy ϕ_t of $\mathbb{P}^2$ to follow changes in the preimage of the self-intersection set (Section 4).

Section 1 contains smoothly immersed models for $i_{b^\pm}$ and $i_{g^\pm}$. In the tradition of Boy's seminal work, these are presented descriptively as the level curves of a non-degenerate height function [5]. We also reconstruct the preimage of the self-intersection set which amplifies the difference in i_b and i_g. In contrast, the differences in the level curve morphologies are so subtle as to seem insignificant. (It is likely that i_g has been unwittingly constructed many times, e.g. [12].) In Sections 2 and 3 we describe restrictions on the self-intersection set and its preimage for a generic immersion. These preimages then provide us with an (essentially cellular) "***immersion-adapted***" decomposition of $\mathbb{P}^2$. Section 3 contains an analysis of adapted decompositions which significantly reduce the possible configurations for the self-intersection set in the image. In Section 4 we describe the $C^\infty(\alpha, T)$-*deformation* of a given immersion which bifurcates a triple point to a pair of pinch points (i.e. Whitney umbrellas). This is a combination of standard Morin–Roseman moves [17]. The resulting non-immersive mapping $j : \mathbb{P}^2 \to \mathbb{S}^3$ is ambiently isotopic to the *crosscap mapping* of the projective plane whose image is the "sphere with a crosscap". This mapping $j : \mathbb{P}^2 \to \mathbb{S}^3$ is unique up to ambient isotopy. (There are two such ambient isotopy classes in $\mathbb{R}^3$.) Since the (α, T)-deformation has localized support in $\mathbb{P}^2$ and is "reversible", Theorem 4.3 will follow from a classification of distinct passages from a given immersion to the crosscap mapping j. The paper closes with simple applications of the theorem: discrete ambient automorphism groups; image-homology of immersions with one triple point; and almost tight ambient isotopy classes.

1. The models

1.1. Three critical point models

The objective of this section is to present simple concrete constructions of C^∞ immersions of $\mathbb{P}^2$ into $\mathbb{S}^3$ for subsequent reference. As in Boy's original work, these are presented descriptively as a sequence of planar level curves of a linear height function $h : \mathbb{R}^3 \subseteq \mathbb{S}^3 \to \mathbb{R}$ whose value, or "height", increases as one moves "upward". It was Boy's insight that, given such a family of level curves, one can construct an essentially unique immersion. For an introduction to this technique, we recommend [12] Fig. 1, where the reader will find a view of Boy's immersion very much like our Fig. 1.1. For more on the subtleties of this methodology as well as details on techniques, we refer the reader to the literature [6,8,13].

The models presented in i_{b^+} (Fig. 1.1) and i_{g^-} (Fig. 1.2) illustrate the main ingredients in the proof of Theorem 4.3. We have chosen i_{b^+} and i_{g^-} for ease of visual comparison. (See the remark at the end of this section for a definition of the $\pm$ designation.) In the center of each of Figs. 1.1 and 1.2 is a sequence of curves representing the structural changes in level curves with three critical points labeled *mx*, *s* and *mn*. These levels are interpolated by standard generic moves found in the literature cited above. The interpolated collection is arranged so as to roughly correspond to the appropriate height in the surface to the right.

The caps immediately above the minimum height and below the maximum are the same in i_{b^+} and i_{g^-}, and are topologically the same as in Fig. 5.1. Descending from the maximum height notice that the only difference in i_{b^+} and i_{g^-} is that the inward-pointing loop in the level curve, which is generated by the saddle point, travels in two distinct ways (as indicated by the arrows) until it points "outward". In these models, it is the loops' distinct ways of travel which correspond to the different twist in the loop of double points lying between the maximum height and the triple point. Locally, one can visualize the surface as a tube attached to the surface along a curve of double points (dotted curve), passing through the surface at the triple point. (Compare with Boy's Figs. 15, 17a, 17b [3].)

The bold curve in the left side of each figure is the preimage of the self-intersection set in the standard plane model for $\mathbb{P}^2$. This preimage is also known as the *double decker set*: the closure of the preimage of the double point set [7].

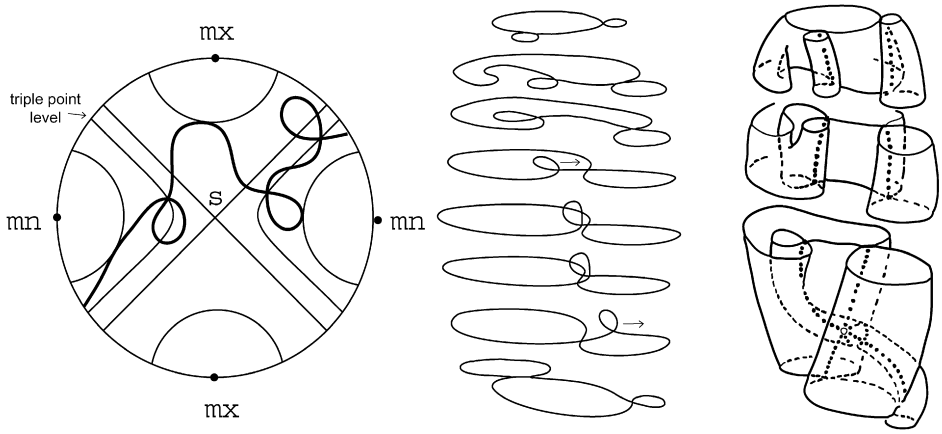

Fig. 1.1. Boy's surface i_{b^+}.

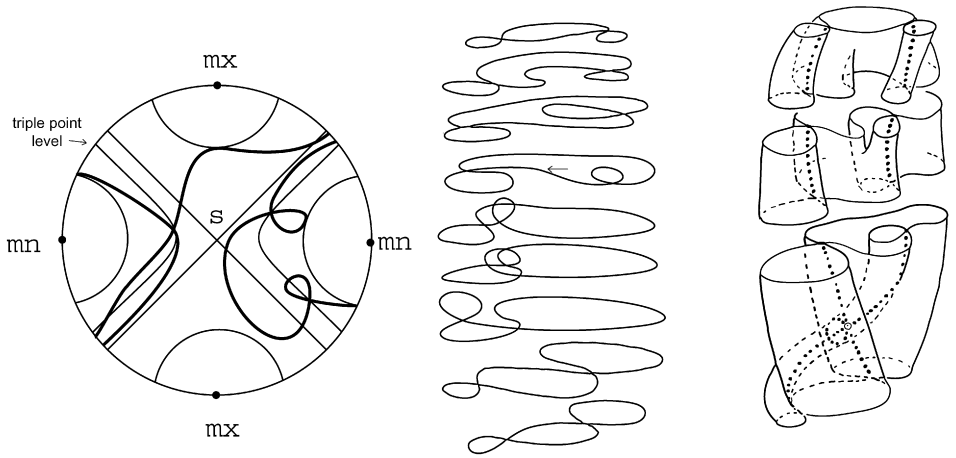

Fig. 1.2. i_{g^-} immersion.

Consider the loop in the self-intersection set $\mathcal{S}_1$ which lies between the maximum height and the triple point height. In the i_{b^+}-model it is filled in by a disk (facing the viewer) in the surface. However in the i_{g^-}-model, the saddle-defined orifice is surrounded by this loop, and hence there is no filling-disk facing the viewer. The only other possibility is that such a disk would be hidden behind the surface but upon inspection such a disk would extend below the triple point and hence its boundary would interact with the other loops in $\mathcal{S}_1$. Thus it cannot be filled in by the image of a disk. In both cases, the remaining loops in $\mathcal{S}_1$ are clearly filled in by such disks. The disk bounded by the small loop is hidden from any viewpoint, whereas the other loop bounds a disk facing the viewer. These disks are much more transparent when examining the preimage of $\mathcal{S}_1$.

We will denote the preimage of $\mathcal{S}_1$ (the double decker set) by $D \subseteq \mathbb{P}^2$. The following paragraph indicates how the homotopy type of D can be inferred from the level curve decomposition. At the left of Figs. 1.1 and 1.2, we use the disk model of $\mathbb{P}^2$ (that is, the disk with antipodal points identified). The height levels in the preimage are drawn as hyperbola-like curves in the disk, and the critical levels, *mx* and *mn*, correspond to pairs of antipodal points. To see that the bold curves in the disk models correspond to D (which in both cases is a C^∞ immersed non-imbedded curve), observe that the induced height function on $\mathcal{S}_1$ will have six non-degenerate critical points, with heights $h_1, h_2, \ldots, h_6$, where D must be tangent to the level curves in $\mathbb{P}^2$. We have implicitly assumed that these critical points are not at the height of the triple point or the saddle point. Descending from the *mx* height to h_6, there are no such tangencies; at h_6 there is one; and between h_6 and h_5 the level curves transversely intersect D precisely four times. Continuing in this fashion produces the level set decomposition for D (presented on the left of Figs. 1.1 and 1.2).

Our strategy for proving Theorem 4.3, as detailed in Section 3, is to construct a decomposition of $\mathbb{P}^2$ adapted to the double-point set of a given immersion and then use topological restrictions to show that it must be diffeomorphic to one of the above two models. The desired ambient isotopy is constructed in Section 4.

The $\pm$ designation on these models for $i_{b^\pm}$ and $i_{g^\pm}$ is determined as follows. A collar neighborhood of the immersed circle of double points is a Möbius band with either a left-handed or right-handed twist (that is, the crossing number of a projection of the boundary curve is negative or positive) [14,16]. The $+$ sign indicates a right-handed (positive) twist and the – sign a left-handed (negative) twist.

1.2. $\mathbb{Z}_2$ rotationally symmetric models in $\mathbb{S}^3$

In this section we will change the level curve decomposition above to construct alternative models for $i_{b^\pm}$ and $i_{g^\pm}$ which have 2-fold rotational symmetry about a great circle axis in an equatorial $\mathbb{S}^2$. On the complement of a 3-ball at ∞ in $\mathbb{S}^3$ the immersions are given by the level curves in Figs. 1.3 and 1.4 respectively, where the equatorial $\mathbb{S}^2$ is represented by the plane of symmetry and the great circle axis of rotation is represented by a vertical line (whose intersection with various levels is shown as black dots down the center in the right-hand portion of the figure). Note that the viewer's line of sight is orthogonal to the equatorial plane of symmetry so all of the cusps in the contour curve must lie on the axis of symmetry.

In a 3-ball at ∞, these immersions agree with the equatorial $\mathbb{S}^2$ and the level curves extend to define an isolated singularity of index 2 (bipole singularity). Since the remaining level curve singularities have index $+1$ at the local maximum and -1 at the two saddles, both level curve morphologies represent immersions of the projective plane.a Descending from ∞, a dome forms in both models, and then two saddles. Notice, however, that the saddles form "inside" vs. "outside" the dome. In contrast to the "loop movement" of the 3-critical-point models (Figs. 1.1, 1.2), on the symmetric models these "saddle locations" provide a distinguishing feature.

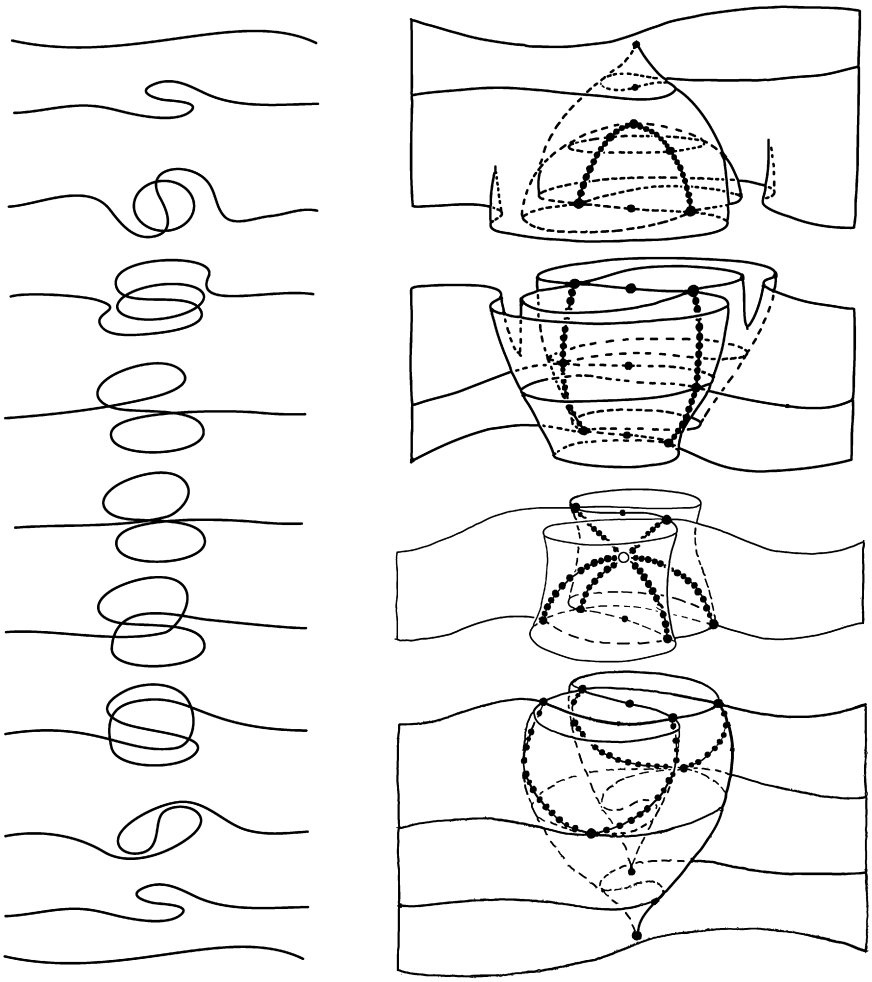

Fig. 1.3. Symmetric i_b immersion.

The two loops of $\mathcal{S}_1$ (bold and dotted in the right of Figs. 1.3, 1.4) which lie below the triple point are clearly spanned by immersed disks. The spanning disk in the vertical loop is clearly spanned by an immersed disk in Fig. 1.3. However in Fig. 1.4 the two saddle points obstruct such a disk.

2. The self-intersection set

Our methods can be described as C^0-cellular topology motivated by, and adapted to, the C^∞ generic setting. Thus we will typically present C^1 models for our C^∞ objects and assume that the models have been perturbed to be C^∞. Let $i:\mathbb{P}^2\to\mathbb{S}^3$ denote a generic immersion of the projective plane into the 3-sphere, and let $\mathcal{S}=i(\mathbb{P}^2)$. Then $\mathcal{S}_1\subset\mathcal{S}\subset\mathbb{S}^3$ is a stratification where $\mathcal{S}_1$ is the (1-dimensional) self-intersection set of the immersion. Let $D=i^{-1}(\mathcal{S}_1)$, and note that the immersion is injective when restricted to $\mathbb{P}^2-D$. We will assume that $\mathcal{S}_1$ is connected and contains exactly one triple point T, hence $\mathcal{S}_1-T$ as a 1-chain consists of three loops (β,γ and δ) of double points each of which begins and ends at T, where they fail to immerse (since the tangents of a loop do not line up at T). The preimages of β,γ and δ are pairs of C^∞ imbedded arcs with disjoint interiors: $i^{-1}(\beta)=\beta_1\cup\beta_2$, $i^{-1}(\gamma)=\gamma_1\cup\gamma_2$, $i^{-1}(\delta)=\delta_1\cup\delta_2$. The preimage of the triple point T consists of three points: T_1, T_2, T_3. Thus D is a collection of (at most three) C^∞ imbedded closed curves in $\mathbb{P}^2$, with each pair intersecting (transversely) precisely at T_1, T_2 or T_3. The three possible configurations of $\mathcal{S}_1$ (viewed as abstract 1-chains containing designated immersed cycles) are shown in Figs. 2.2–2.4 below. A neighborhood V of the triple point T in $\mathcal{S}$ is shown in Fig. 2.1. Label the "*opposite*" ends of the double point arcs in V by $z_\pm, y_\pm, x_\pm$ respectively. We will refer to the remaining pairs as "*adjacent*" ends. For example, x_+ is adjacent to $y_\pm$ and $z_\pm$.

A priori, the self-intersection set $\mathcal{S}_1$, as an abstract 1-chain, must consist of one, two or three immersed closed curves which may become knotted when realized as a self-intersection set in $\mathbb{S}^3$. Specifically, the cases (illustrated in Figs. 2.2–2.4) are as follows:

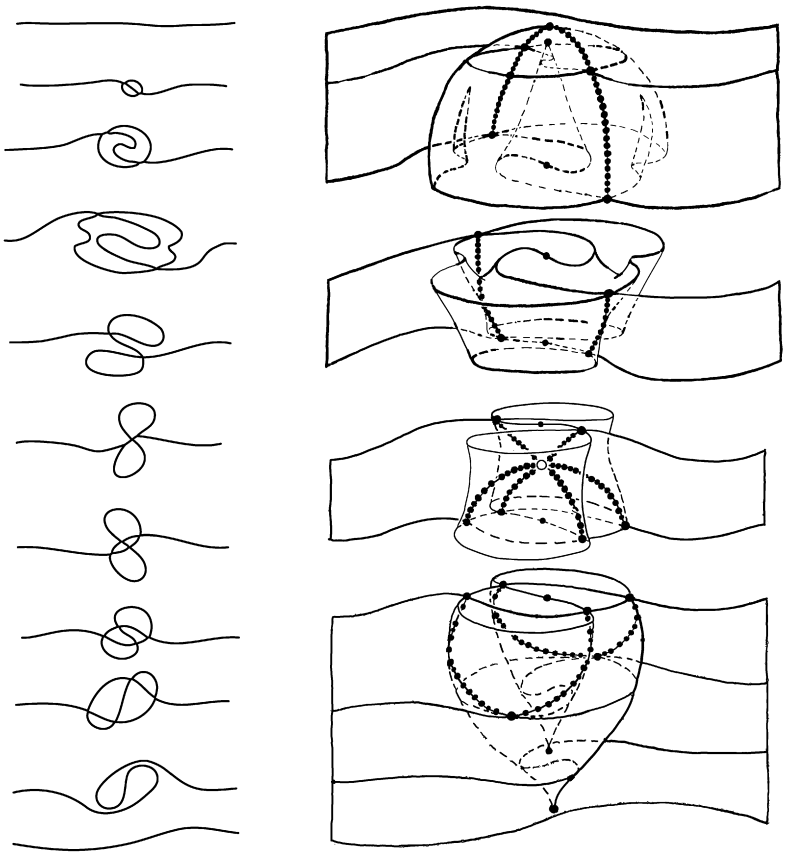

Fig. 1.4. Symmetric i_g immersion.

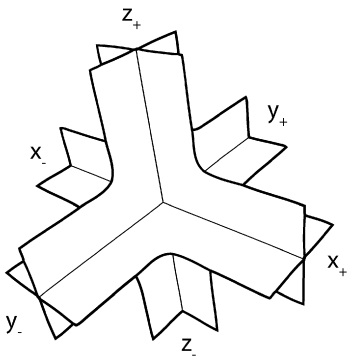

Fig. 2.1.

Case I. *Three immersed loops in $\mathcal{S}_1$ passing through T* The loops are obtained from V by connecting z_+ to z_-, x_+ to x_-, and y_+ to y_-.

Case II. *Two immersed loops in $\mathcal{S}_1$ passing through T* One loop is obtained by connecting the $+$ and $-$ ends of one axis, say z_+ to z_-. The other loop is a figure-eight obtained by connecting x_+ to either y_+ or y_-, and x_- to the remaining end.

Case III. *$\mathcal{S}_1$ consists of a single immersed circle* The circle is obtained by connecting x_+ to y_-, y_+ to z_-, and z_+ to x_-.

We will refer to these standard 1-chain configurations in Section 3, where we construct the immersion-adapted decompositions of $\mathbb{P}^2$, and use them to eliminate Cases I and II from occurring in an immersion of $\mathbb{P}^2$ with one triple point.

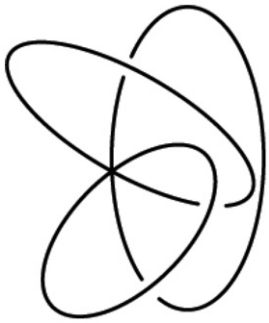

Fig. 2.2.

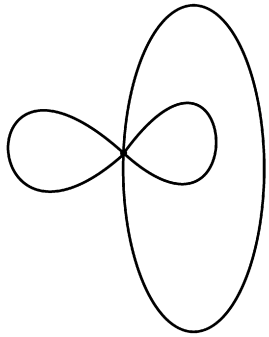

Fig. 2.3.

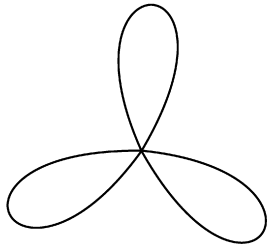

Fig. 2.4.

3. Immersion-adapted decompositions of $\mathbb{P}^2$

Throughout this section, we are given a C^∞ generic immersion $i:\mathbb{P}^2\to\mathbb{S}^3$ satisfying the hypotheses of Theorem 4.3 (the self-intersection set in $\mathbb{S}^3$ is connected and has a single triple point). We now show that Cases I and II of Section 2 cannot occur as the self-intersection set of such an immersion, and that Case III yields two precisely two adapted decompositions up to a diffeomorphism of $\mathbb{P}^2$. We begin by describing some general restrictions on connecting ends of the neighborhood V (Fig. 2.1). Note that the connections could insert twists in V when realized in $\mathbb{S}^3$.

Lemma 3.1. *If opposite ends of V are connected then this connection must have an odd number of quarter-twists. If adjacent ends are connected, then this connection must have an even (possibly 0) number of quarter-twists.*

Proof. Recall that $\mathcal{S}-\mathcal{S}_1$ admits a normal vector field in $\mathbb{S}^3$, i.e., $\mathcal{S}-\mathcal{S}_1$ has a consistent transverse orientation in the sense of [3,12]. (Essentially, the complement of $\mathcal{S}$ can be divided into two families according to whether geodesic rays from a fixed point in the complement meet $\mathcal{S}$ in an even number or an odd number of points. One family can then be designated as the positive side of $\mathcal{S}$.) The lemma is a restatement of conditions on connected ends so as to admit such a vector field. □

Corollary 3.2. *If opposite ends of V are connected to create an immersed loop in $\mathcal{S}_1$, then the preimage of the loop is the core of a Möbius band in $\mathbb{P}^2$.*

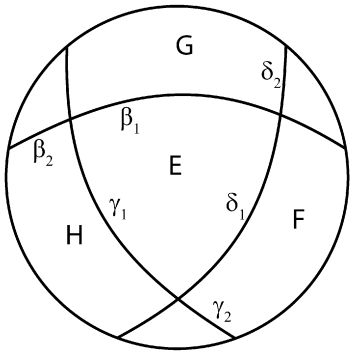

Fig. 3.1.

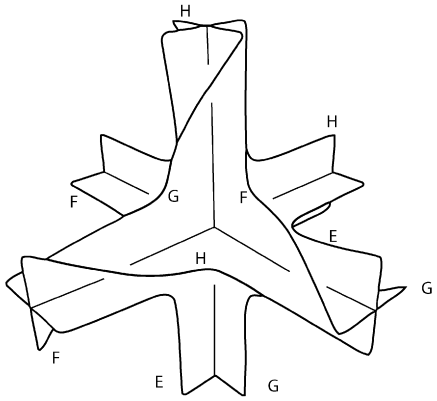

Fig. 3.2.

Proof. Without loss of generality, we may assume z_+ is connected to z_- by an arc ε in $\mathcal{S}_1$. Let C denote a "*cross*": $\{(x, y) \in [-1, 1] \times [-1, 1] \mid xy = 0\}$. A tubular neighborhood of ε in $\mathcal{S}$ is homeomorphic to $C \times I$, where $I = [0, 1]$. By Lemma 3.1, there must be an odd number of quarter-twists in $C \times I$ as it connects z_+ to z_- in $\mathbb{S}^3$. This defines an immersion of the Möbius band $\mathbb{M}$ into $\mathcal{S}$ so that the core circle c double covers the loop. Hence, the preimage must be a loop in $\mathbb{P}^2$ with a neighborhood homeomorphic to a Möbius band. □

Now we begin the analysis which will eliminate all but one of the three possible 1-chain configurations presented in Section 2. We will denote the intersection of $\mathcal{S}$ in $\mathbb{S}^3$ with a tubular neighborhood of $\mathcal{S}_1$ by $\widehat{V}$. This should be thought of as V (Fig. 2.1) with its ends appropriately identified.

Proposition 3.3. *Case* I*, in which $\mathcal{S}_1$ consists of three immersed, imbedded transverse components through T, cannot be realized as the self-intersection set of i in $\mathbb{S}^3$.*

Proof. Let β, γ, and δ be the components of $\mathcal{S}_1$. By Corollary 3.2, the preimage of each component (i.e., the concatenations $\beta_1\beta_2$, $\gamma_1\gamma_2$, or $\delta_1\delta_2$) is an orientation-reversing loop in $\mathbb{P}^2$ double-covering its image loop. Further each preimage intersects precisely at two of the three preimages of T. That is, D is homeomorphic to the configuration shown in the plane model of $\mathbb{P}^2$ in Fig. 3.1.

The complement of a collar neighborhood of D consists of four disks: E, F, G, H. The corresponding neighborhood $\widehat{V}$ of $\mathcal{S}_1$ in $\mathcal{S}$ must be as in Fig. 3.2. Each edge is labeled according to the disk it bounds in $\mathbb{P}^2$ and end identifications are dictated by the labels on the boundary curves of the four disks. There may be additional full 360°-degree twists along any of the loops, but this does not affect the labeling of the edges of $\widehat{V}$.

Since each edge of $\widehat{V}$ bounds an imbedded disk in $\mathcal{S}$, it is unknotted in $\mathbb{S}^3$. We claim that each of the loops β, γ and δ is also unknotted. Suppose β is knotted; then it has a locally knotted arc in $\mathbb{S}^3 - \widehat{V}$. However then an edge of $\widehat{V}$ would also have a locally knotted arc, and hence is a composite knot. Additivity of the genus [18] would then imply that this edge cannot be the unknot, a contradiction.

Therefore β is unknotted and hence bounds a disk Δ in $\mathbb{S}^3$. Put Δ in general position so that $\mathcal{S}$ meets Δ transversely. The set $\mathcal{S} \cap \Delta$ is a graph. Each interior vertex, where Δ is transverse to $\mathcal{S}_1$, is 4-valent. Further, from Fig. 3.2, we note that at each such intersection with $\mathcal{S}_1$, the four faces emanating from the vertex have distinct labels (E, F, G, or H).

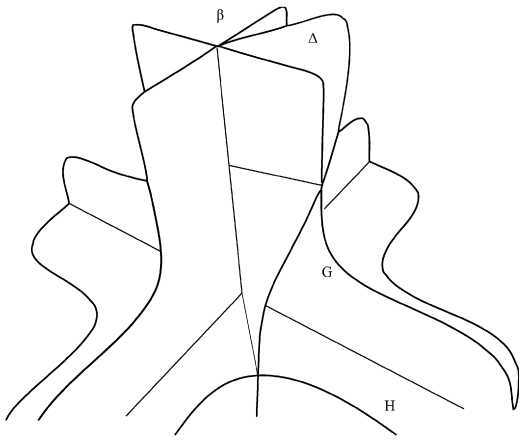

Fig. 3.3.

There must be at least two arcs of intersection with $\mathcal{S}$ that meet the boundary of Δ: one resulting from the intersection of Δ with the "xy"-plane through T in Fig. 3.3, and the other from the necessary twist along the "z"-axis. Without loss of generality, we can take those arcs to be labeled G and H.

First, assume these are the only arcs of $\mathcal{S} \cap \Delta$ meeting the boundary of Δ. This is equivalent to assuming there are no 360°-degree twists in the loop β. Let $\mathcal{K}$ be the subgraph of $\mathcal{S} \cap \operatorname{int} \Delta$ connected to these two arcs. The vertices of $\mathcal{K}$ arise from intersections with $\mathcal{S}_1$. Suppose there are m such vertices. Counting the number of edges emanating from each vertex of $\mathcal{K}$, we get

$e =$ number of edges coming from intersection with face $E = m/2$,

$f =$ number of edges coming from intersection with face $F = m/2$,

$g =$ number of edges coming from intersection with face $G = (m+1)/2$,

$h =$ number of edges coming from intersection with face $H = (m+1)/2$.

But $e = m/2$ implies that m is even, while $g = (m+1)/2$ implies m is odd. Therefore this case cannot occur.

Now suppose there are some 360°-degree twists along β. Each such twist adds four additional edges of $\mathcal{K}$ meeting the boundary of Δ, one with each of the four face labels. Hence each such twist adds 1 to the numerator of each of e, f, g and h, and the parity problem persists.

We conclude that Case I, in which $\mathcal{S}_1$ is diffeomorphic to three immersed loops through T, cannot occur. □

It is interesting to note that this case *can* occur in $\mathbb{S}^3/Q$ where Q is the quaternionic group of order 8 [6].

Proposition 3.4. *Case* II*, in which $\mathcal{S}_1$ consists of two loops, one immersed and imbedded and one immersed but not imbedded, cannot be realized as the self-intersection set of i in $\mathbb{S}^3$.*

Proof. One of the smooth loops in $\mathcal{S}_1$ is obtained by connecting the positive and negative ends of one axis, say z_+ to z_-. Call this loop δ. The other smooth loop is a figure-eight obtained by say connecting x_+ to y_+ (call this arc β) and x_- to y_- (call this arc γ). The preimage D is homeomorphic to the 1-chain shown in Fig. 3.4.

Corollary 3.2 implies that the preimage of δ (labeled $\delta_1\delta_2$ in the figure) is an orientation-reversing loop with a Möbius band neighborhood which double-covers δ. The complement of this Möbius band in $\mathbb{P}^2$ is a disk. Up to diffeomorphism, the only way the above 1-chain can be imbedded in $\mathbb{P}^2$ is as shown in Fig. 3.5 (i.e., there is only one way to imbed the Möbius band, hence $\delta_1\delta_2$, and the imbedding of the remainder of the 1-chain is determined). The figure-eight component lies in one of the three complementary disk faces.

Thus the complement of a collar neighborhood of D in $\mathbb{P}^2$ would have six boundary components. We will now show this cannot occur. Notice that, since the figure-eight component lies in a disk in $\mathbb{P}^2$, there can be no twists realized in its collar neighborhood. Hence when we connected the ends of V to create $\widehat{V}$, the only twisting along β or γ must be 360° twists, and 360° twists do not affect the number of boundary components of $\widehat{V}$. Similarly, although we know there must be at least one quarter-twist along δ, any additional 360° twist has no effect on the number of boundary components. Counting the number of boundary components in $\widehat{V}$ with a quarter-twist along δ, we see there can be only four, not six as shown in Fig. 3.5. Thus Case II cannot be realized. □

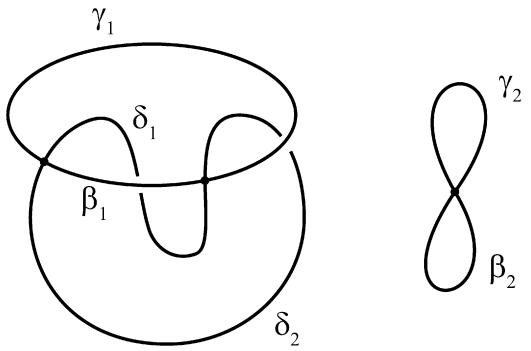

Fig. 3.4.

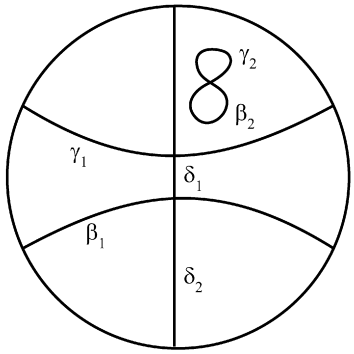

Fig. 3.5.

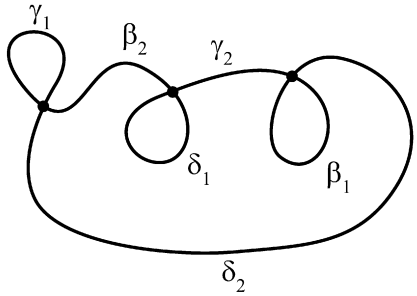

Fig. 3.6.

Proposition 3.5. *Case* III*, in which $i(D) = \mathcal{S}_1$ consists of one immersed cycle, the preimage D has precisely two possible configurations up to diffeomorphism of $\mathbb{P}^2$ (Figs.* 3.8 *and* 3.9*), each of which is realizable as the self-intersection set of an immersion satisfying the hypotheses of Theorem* 4.3*.*

Proof. Without loss of generality (up to a reflection in $\mathbb{S}^3$), we may assume that the immersed cycle is created by identifying x_+ to y_-, y_+ to z_-, and z_+ to x_-. In this case D is homeomorphic to the 1-chain $\mathcal{N}$ shown in Fig. 3.6.

At least one loop in this 1-chain must be homotopically non-trivial in $\mathbb{P}^2$. Otherwise the complement of $\mathcal{N}$ contains a Möbius band and hence there would be an imbedded Möbius band in $\mathcal{S} - \mathcal{S}_1$, contradicting transverse orientability as in the proof of Lemma 3.1. So either

Case B: the loop $\beta_2\gamma_2\delta_2$ in $\mathcal{N}$ is homotopically non-trivial or
Case G: at least one of the loops β_1, γ_1, or δ_1 is homotopically non-trivial.

To show there are the only two possible ways to realize Cases B and G, note that the preimage in $\mathbb{P}^2$ of the neighborhood V of the triple point T consists of three components, each homeomorphic to a neighborhood of one of the three preimages of T, as shown in Fig. 3.7. Information about how the ends of these components are identified will allow us to reconstruct D as a subset of $\mathbb{P}^2$.

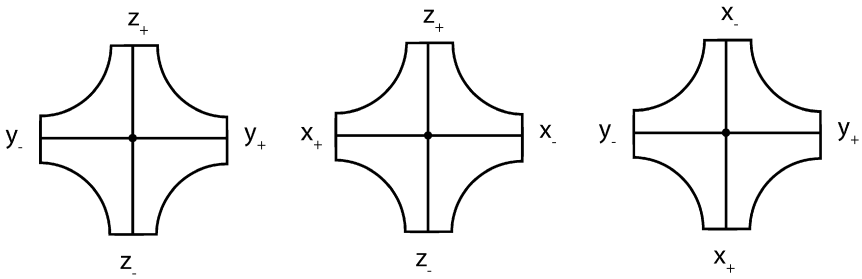

Fig. 3.7.

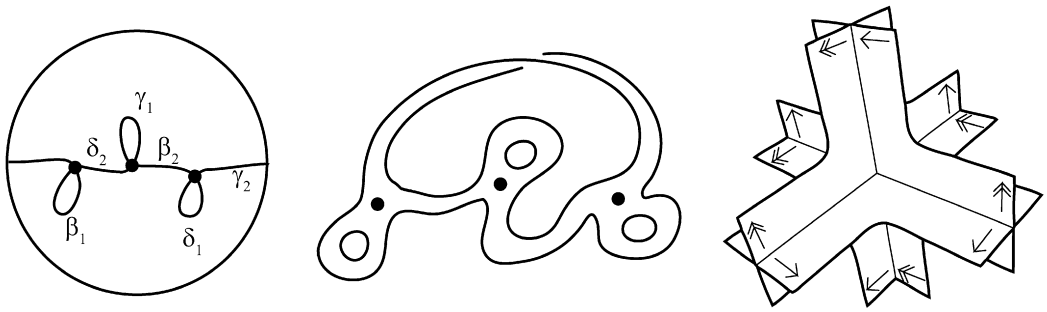

Fig. 3.8. Case (B).

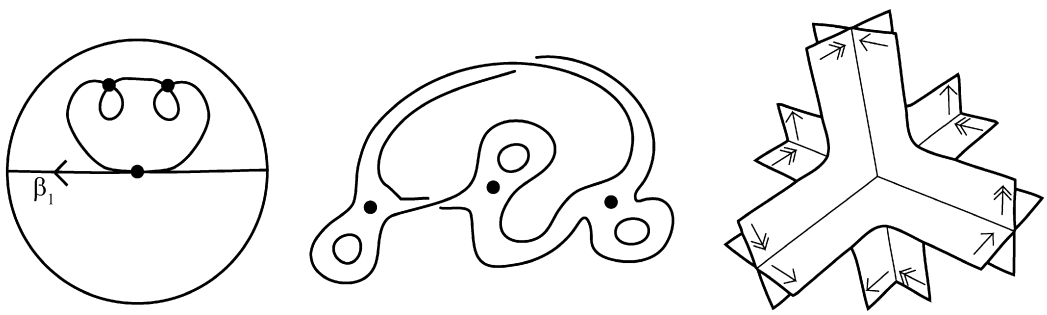

Fig. 3.9. Case (G).

Fig. 3.10.

Case B. Without loss of generality, assume the loop $\beta_2\gamma_2\delta_2$ in $\mathcal{N}$ is essential in $\mathbb{P}^2$. The complement of this loop is a disk so the loops β_1, γ_1, and δ_1 must bound disks in $\mathbb{P}^2$. Their image loops β, γ, δ bound imbedded disks in $\mathcal{S}$, hence we have the ends of V connected with orientations as shown at the left in Fig. 3.8. That is to say the collar neighborhood of D is created by connecting the ends of the components of $i^{-1}(V)$ in Fig. 3.7 according to the specified connection rules, which in turn determines how the set D must imbed in $\mathbb{P}^2$. Notice that, since the complement of $\beta_2\gamma_2\delta_2$ is a disk, up to diffeomorphism there is only one way to imbed the Möbius band, and hence $\beta_2\gamma_2\delta_2$. The imbedding of the remainder of the 1-chain is determined and there is no choice as to how the rest of D imbeds in $\mathbb{P}^2$ (Fig. 3.8).

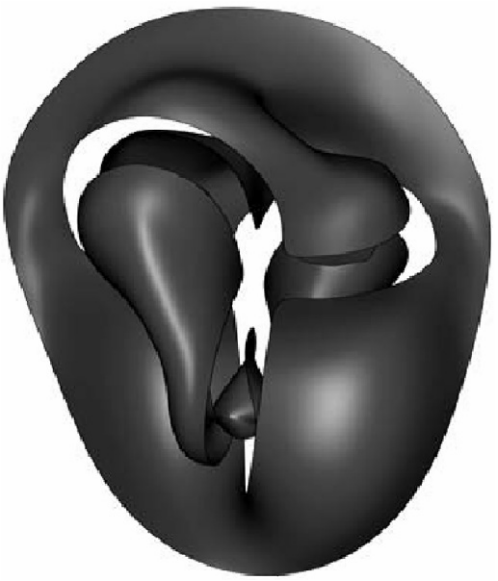

Fig. 3.11.

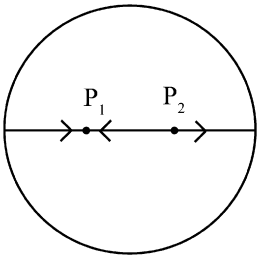

Fig. 4.1.

Case G. Without loss of generality, assume β_1 is homotopically essential in $\mathbb{P}^2$. As in Case 1, we argue that γ_1, δ_1 bound disks in $\mathbb{P}^2$, hence γ and δ again bound imbedded disks in $\mathcal{S}$. The imbedding of D in $\mathbb{P}^2$ and a collar neighborhood of D are shown in Fig. 3.9. The resulting connections rules for V are also shown. Note that the axis-orientation of V is the same as in Fig. 2.1.

Both of the above are realizable in $\mathbb{S}^3$, as they are diffeomorphic to D for i_{b^+} and i_{g^+} as indicated in Figs. 1.1 and 1.2 in Section 1. Stages of the construction of (B) are well known (e.g., Figs. 1.5, 1.6 [8]). Stages of the construction of less known Case (G) are illustrated in Fig. 3.10. The surface in Fig. 3.11, with one disk and a neighborhood of the self-intersection set removed, is ambiently isotopic to i_g. For more of Mellnik's CAD renderings and animations of i_b and i_g, see the link at www.math.unc.edu/Faculty/seg. □

4. Proof of the main theorem

It remains to be shown that any immersion i with $D = i^{-1}(\mathcal{S}_1)$ diffeomorphic to Case (B) or (G) is ambiently isotopic to $i_{b^\pm}$ or $i_{g^\pm}$. Since we want to follow the creation, destruction and movement of the pinch points in the image and preimage, we now define the notion of a deformation arc. See Figs. 4.2–4.4 for illustrations of the procedure described below.

First we use these preimages to construct an $(\boldsymbol{\alpha}, \mathbf{T})$-***deformation*** $j_t : \mathbb{P}^2 \to \mathbb{S}^3$, $t \in [0, 1]$, where $j_0 = i$, and where $j_1 = j$ is the non-immersive crosscap mapping whose image is the "sphere with a crosscap" (see [12], Section 3 for an explicit parametrization). The mapping j has an arc of double points terminating in a pair of pinch points, P_1 and P_2, and no triple points. The preimage of the arc of double points is an non-trivial curve D' marked by the preimages of the pinch points (also denoted P_1 and P_2) as in Fig. 4.1. The map j is unique up to ambient isotopy (i.e. a neighborhood of D' has image diffeomorphic to the dehomogenized Plucker conoid [9] intersected with a 3-ball and, in $\mathbb{S}^3$, there is only one way to attach an imbedded disk to its boundary). The (α, T)-deformation will determine a ***deformation arc*** in $\mathbb{P}^2$ which joins the preimages of the pinch points and transversely intersects $D' - \{P_1, P_2\}$ in exactly one point. This deformation process is reversible; that is, given such a deformation arc for D' in $\mathbb{P}^2$, there is a deformation j_t such that j_0 is an immersion with exactly one triple point, and j_0 is unique up to ambient isotopy.

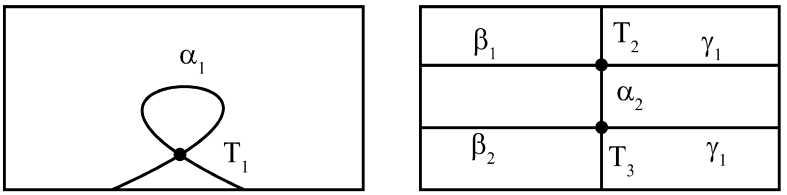

Fig. 4.2.

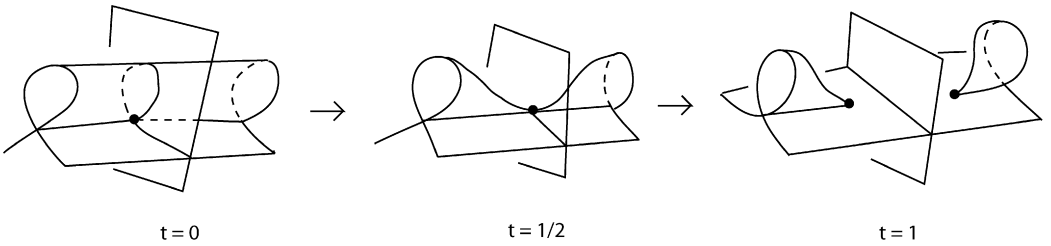

Fig. 4.3.

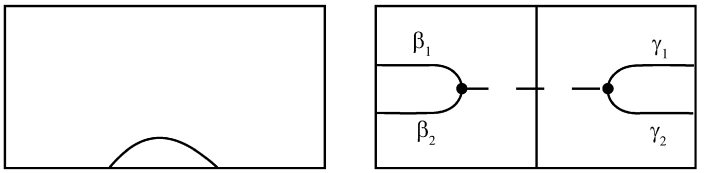

Fig. 4.4.

The (α, T)-deformation will be locally supported and can be defined for any generic immersion i with an "*α-loop*" in $\mathcal{S}_1$ which contains a triple point T (i.e., a loop in $\mathcal{S}_1$ which is the boundary of an imbedded disk $i(\Delta)$ in $\mathcal{S}$, and this boundary contains T). In this setting, the loop has two preimages, α_1 and α_2. One, say α_1, is a loop through T_1 in $i^{-1}(T)$ which bounds a disk in $\mathbb{P}^2$. The other, α_2, is an arc in $\mathbb{P}^2$ joining the other two preimages of T (call them T_2 and T_3). Let β and δ denote the other arcs entering and leaving $i^{-1}(T)$. Locally, in $\mathbb{P}^2$, we have Fig. 4.2.

The deformation j_t will have support on a neighborhood of α_2 where it has local representation $j_t(u, v) = (u, v^2, v^3 - v(u^2 + 2t - 1)) = (x, y, z)$ with α_2 represented by the unit interval on the v-axis and $i(\Delta)$ lies in the $x = 0$ plane. The image is as in Fig. 4.3.

During the (α, T)-deformation, the preimage of the self-intersection set changes as follows: as t approaches $\frac{1}{2}$, the α-loop contracts to the point T and then disappears. The j_t-preimage of its double-point set changes as follows: as t approaches $\frac{1}{2}$, α_1 and α_2 shrink to points; at $t = \frac{1}{2}$, β_i and γ_i all join; and for $t > \frac{1}{2}$, β_1 and β_2 join at the preimage of one pinch point; γ_1 and γ_2 at the other. Compare Figs. 4.2 and 4.4.

With the following two propositions we will have a proof of Theorem 4.3.

Proposition 4.1. *For each immersion $i_{b^\pm}$ and $i_{g^\pm}$, there exists an (α, T)-deformation taking the immersion to the crosscap mapping.*

Proof. Note that composing an immersion with a diffeomorphism of $\mathbb{S}^3$ does not change the preimage of the self-intersection set so we need only prove the $+$ cases.

The loop labeled γ in the proof of Proposition 3.5 is an α-loop. Since $\mathcal{S}_1$ is a single immersed circle, the (α, T)-deformation constructed on γ transforms $\mathcal{S}_1$ into an arc of double points, with each end terminating in a pinch point. In each case, we trace the deformation path in the preimage for use later. The preimage deformations are shown in Fig. 4.5, where the deformation arcs are indicated by a dashed curve. The grey dot indicates the point at which the α-loop (γ_1) vanished. In each case, the deformation results in the double-point set D' for the crosscap mapping, but with distinct deformation arcs. □

Define an ***allowable deformation arc*** in the preimage of the crosscap map j to be an arc joining the pinch point preimages and crossing D' transversely exactly once. We will say two deformation arcs are ***equivalent*** if one can be homotoped in $\mathbb{P}^2$ to the other staying within the class of allowable deformation arcs.

Proposition 4.2. *Any allowable deformation arc for the crosscap mapping is equivalent to one of the deformation arcs in Proposition 4.1, or its mirror image.*

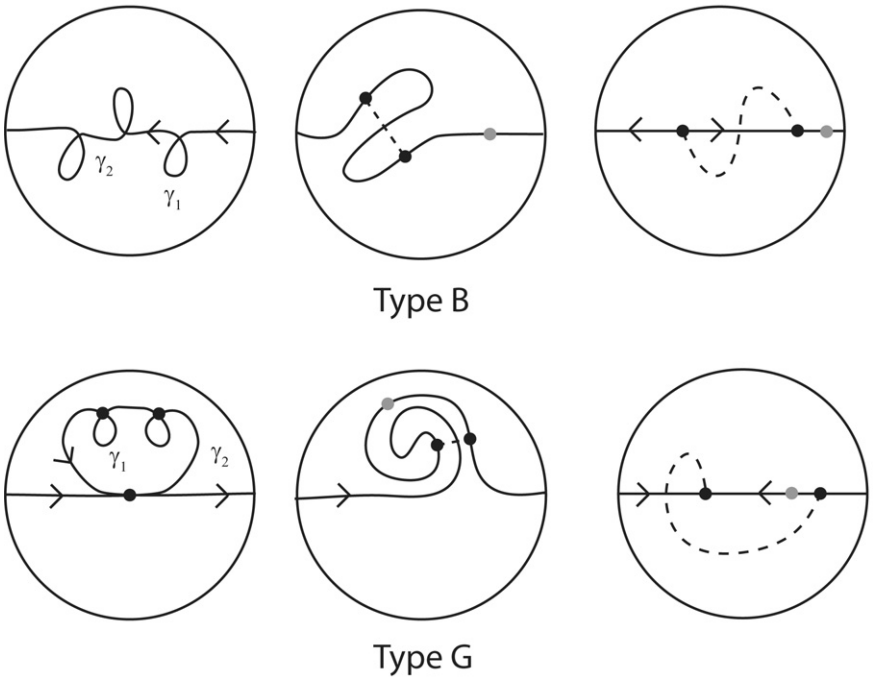

Fig. 4.5.

Proof. Let $\widetilde{\Delta}$ be the standard planar model for $\mathbb{P}^2$, i.e., a disk with its boundary identified by the antipodal map. Let the horizontal diameter of $\widetilde{\Delta}$ be the preimage D' of the self-intersection set for the crosscap mapping j. Orient the self-intersection set and give D' the inherited orientation. Denote the pinch point preimages by P_1 and P_2 with P_1 being the point with inward oriented segments on either side. There is an induced orientation on the deformation path μ going from P_1 to P_2. (See Fig. 4.1.) There are exactly four homotopy classes of deformation arcs joining P_1 and P_2.

i. As μ leaves P_1 it enters the upper half-disk, crosses D' to the left of P_1 and then joins P_2 in the lower half-disk of $\widetilde{\Delta}$ without crossing the boundary of $\widetilde{\Delta}$.
ii. As μ leaves P_1 it enters the lower half-disk, crosses D' to the left of P_1 and then crosses the boundary of $\widetilde{\Delta}$ before joining P_2. Note that this is equivalent to μ entering the upper half-disk, crossing D' to the *right* of P_1 and then joining P_2 without crossing the boundary of $\widetilde{\Delta}$.
iii. As μ leaves P_1 it enters the lower half-disk, crosses D' to the left of P_1 and then joins P_2 in the upper half-disk of $\widetilde{\Delta}$ without crossing the boundary of $\widetilde{\Delta}$. This is the mirror image of case i.
iv. As μ leaves P_1 it enters the lower half-disk, crosses D' to the left of P_1 and then crosses the boundary of $\widetilde{\Delta}$ before joining P_2. This case is equivalent to the mirror of case ii.

These cases are illustrated in Fig. 4.6. This completes the classification of deformation arcs. □

Thus up to diffeomorphism of $\mathbb{P}^2$ there are but two possible homotopy classes of admissible (α, T)-deformation arcs for the crosscap mapping. It follows that the $\pm$ designation in $i_{b^\pm}$ and $i_{g^\pm}$ cannot be inferred from D in $\mathbb{P}^2$ since the composition of an immersion with a reflection of $\mathbb{S}^3$ has no effect on the preimage.

Theorem 4.3. *If $i : \mathbb{P}^2 \to \mathbb{S}^3$ is a C^∞ immersion with transverse self-intersection, whose self-intersection set in $\mathbb{S}^3$ is connected and has a single triple point then i is ambiently isotopic to $i_{b^\pm}$ or $i_{g^\pm}$.*

Proof. The theorem follows from Propositions 3.3–3.5 and 4.1–4.2 as follows. For any such immersion i, choose a collar neighborhood of the immersed circle of double points which is a Möbius strip with either a left-handed or a right-handed twist. Without loss of generality we will assume that i corresponds to a right-handed twist and will show that it is ambiently isotopic to i_{b_+} or i_{g_+}. The choice of i_{b_+} or i_{g_+} is determined by the preimage of the self-intersection set of i, which must correspond to one of the two configurations in Proposition 3.5. Hence there is an α-loop upon which we can construct an (α, T)-deformation j_t taking i to the crosscap mapping. We may assume that at $t = \frac{1}{2}$ the mapping $j_{1/2}$ bifurcates as in Fig. 4.3. By Proposition 4.2, the deformation arc for this homotopy is equivalent to the deformation arc (i) or (ii) of Fig. 4.6. Now construct j_t^+ for i_{b_+} or i_{g_+} as appropriate; i.e., if the deformation arc is equivalent to (i), construct an (α, T)-

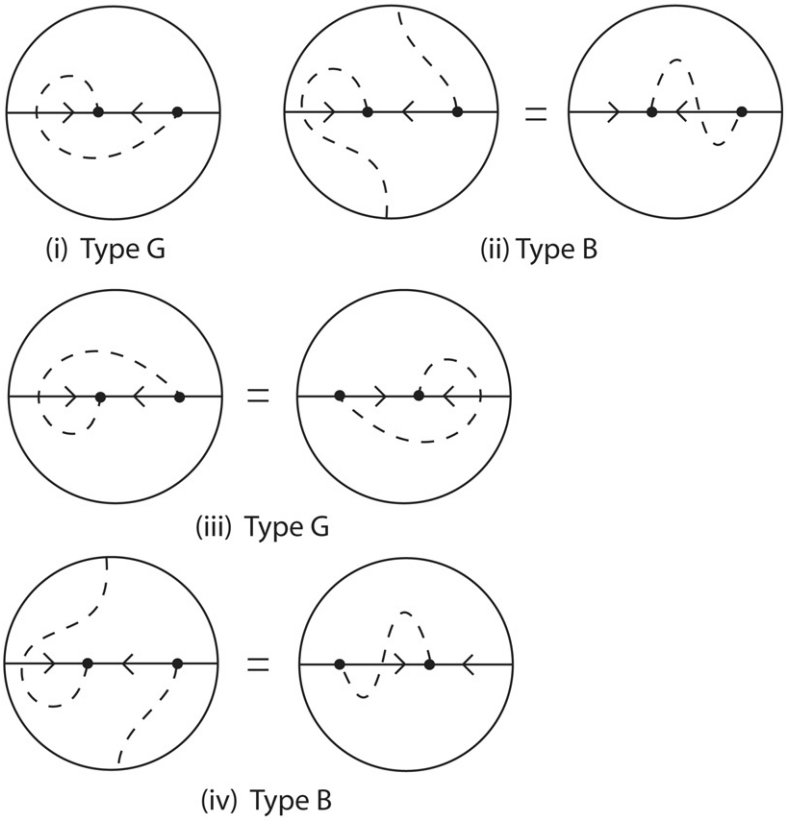

Fig. 4.6.

deformation for i_{g_+}, and similarly for (ii). Since, for t in $[0, \frac{1}{2})$, j_t and j_t^+ can be represented by ambient isotopies and there exists a diffeomorphism Φ^+ of $\mathbb{S}^3$ with $j_{1/2} = \Phi^+ \circ j_{1/2}^+$, a localized surgery modification of the concatenation of j_t and $\Phi^+ \circ j_t^+$, $t \in [0, \frac{1}{2}]$, produces the desired ambient isotopy. □

5. Applications

We close the paper with applications of Theorem 4.3 to the following topics in the differential topology of submanifolds: discrete ambient automorphism groups; image-homology of immersions with one triple point; and almost tight ambient isotopy classes.

5.1. Finite ambient automorphism groups

Here we will distinguish immersions equivalent to $i_{b_\pm}$ or $i_{g_\pm}$ by the groups of orientation-preserving diffeomorphisms of $\mathbb{S}^3$ which leave invariant their image surfaces. At one extreme, *any* vector field on $\mathbb{S}^3$ which is tangent to the stratification $T \subseteq \mathcal{S}_1 \subseteq \mathcal{S}$ defines a flow which preserves $\mathcal{S}$. At the other extreme, it has been shown that the only possible ambient isometry group of a generically immersed projective plane in Euclidean 3-space is cyclic of order 3 [10]. The definition below extracts desirable features of flow automorphisms and geometric symmetries.

Given an immersion $i : \mathbb{P}^2 \to \mathbb{S}^3$ and a finite group Σ, we define a ***i-invariant automorphism action*** by Σ to be an injective group homomorphism $\Lambda : \Sigma \to \mathit{Diff}_+(\mathbb{S}^3)$ which preserves $\mathcal{S} = i(\mathbb{P}^2)$. That is to say, for all σ in Σ, the associated diffeomorphism $\Lambda(\sigma) = \Phi_\sigma : \mathbb{S}^3 \to \mathbb{S}^3$ maps $\mathcal{S}$ to itself. It follows that the stratification $T \subset \mathcal{S}_1 \subset \mathcal{S} \subset \mathbb{S}^3$ must also be preserved: $\Phi_\sigma(T) = T$, $\Phi_\sigma(\mathcal{S}_1) = \mathcal{S}_1$. We say the action is ***T-faithful*** if the homomorphism induced by the differentials at the fixed triple point T, $\Lambda_* : GL(T_T\mathbb{S}^3, \mathbb{R})$, $\Sigma_*(\sigma) = \Phi_{\sigma *} : T_T\mathbb{S}^3 \to T_T\mathbb{S}^3$ is also injective. Such an action is ***maximal*** if $\Lambda(\Sigma) \subseteq \Lambda'(\Sigma') \subseteq \mathit{Diff}_+(\mathbb{S}^3)$ implies $\Sigma = \Sigma'$. Let Sym_n denote the symmetric group on n letters.

Corollary 5.1. *The immersions $i_{b_\pm}$ admit a maximal T-faithful Sym_3-action, and the immersions $i_{g_\pm}$ admit a maximal T-faithful Sym_2-action.*

Proof. Given $i = i_{b_\pm}$ or $i_{g_\pm}$, choose a parametrization of the circle of self-intersection points $\mathcal{S}_1$. This defines three cyclically-ordered unit tangent vectors (v_1, v_2, v_3) in the tangent space of $\mathbb{S}^3$ at T. Let $[v_1]$, $[v_2]$, $[v_3]$ be three corresponding points in the projectivization of $T_T(\mathbb{S}^3)$. Note that since every σ in Σ has finite order, it follows that, if $\sigma \neq id$, then $\Phi_{\sigma *}$ cannot fix these three points. Hence, for any σ in Σ, $\Phi_{\sigma *}$ is determined by the induced permutation of $[v_1]$, $[v_2]$, $[v_3]$. It follows that the largest possible faithful group is Sym_3. However in the case of $i_{g_\pm}$, the loop of $\mathcal{S}_1$ with a half-twist must be invariant under any $i_{g_\pm}$-invariant automorphism, hence the corresponding pair of points in the projectivization must be interchanged by $\Phi_{\sigma *}$ and the largest possible group is Sym_2.

We need only construct the required actions. This should be clear from Boy's 3-fold symmetric model and the 2-fold symmetric models in Section 1. More formally, we have the following constructions for Λ.

For $i = i_{b_\pm}$ there is an ambient diffeomorphism Φ with $\Phi \circ i$ given by Boy's 3-fold symmetric model. Pulling back the 120°-rotation over this diffeomorphism $Rot_3 \circ \Phi^{-1} = \rho_3$ defines a $\mathbb{Z}_3$ action on i generated by ρ_3. The differential at T, $(\rho_3)_*$, "rotates" the points $[v_1]$, $[v_2]$, $[v_3]$. Similarly denote the 2-fold symmetric model of $i_{b_\pm}$ shown in Fig. 1.3 of Section 1 by $\tilde{\Phi} \circ i$ and pull back the 180°-rotation over the diffeomorphism $\tilde{\Phi}$ to define a $\mathbb{Z}_2$ action on i generated by $Rot_2 \circ \tilde{\Phi}^{-1} = \rho_2$. The differential at T, $(\rho_2)*$, exchanges two of the points $[v_1]$, $[v_2]$, $[v_3]$, leaving the third fixed. The action Λ of Sym_3 is now defined by all (compositional) words on the symbols ρ_2 and ρ_3. Similarly for $i_{g_\pm}$ the 2-fold symmetric model in Fig. 1.4 of Section 1 gives rise to an action of Sym_2. □

As a consequence of [10] and Corollary 5.1, we have that no immersion into Euclidean 3-space with non-trivial geometric symmetry can be equivalent to $i_{g_\pm}$, and no immersion into $\mathbb{S}^3$ with order 3 symmetry can be equivalent to $i_{g_\pm}$.

5.2. Homology of the image of immersed projective planes with one triple point

In this section, we extend our classification of immersions of $\mathbb{P}^2$ to allow other components of the self-intersection set, but no additional triple points. Further we compute the $\mathbb{Z}_2$-homology of the image set for such an immersion.

Let $\tilde{i} : \mathbb{P}^2 \to \mathbb{S}^3$ be a C^∞ generic immersion with one triple point T and self-intersection set a disjoint union $\tilde{\mathcal{S}}_1 = \mathcal{S}_1 \cup \mathcal{S}_1'$, where T lies in $\mathcal{S}_1$. Pinkall's quadratic form $q : H_1(\mathbb{P}, \mathbb{Z}_2) = \mathbb{Z}_2 \to \mathbb{Z}_4$ must have support on $D = \tilde{i}^{-1}(\mathcal{S}_1)$ and hence must be trivial on any component $D' = \tilde{i}^{-1}(\mathcal{S}_1')$, [14]. Further a component in D' cannot intersect itself since there is only one triple point whose preimage lies in D, not D'. Thus each component of D' is a simple closed curve. The map $\tilde{i} : D' \to \mathcal{S}_1'$ is 2-to-1 and restricts to an imbedding on each component. The set D' then decomposes into two sets of curves: annular pairs (such that the two preimages of a circle are nested) and disk pairs (such that the two preimage interiors are disjoint). Since D' is finite, there is at least one "deepest" annular pair (i.e. a pair which has no component of D' inside the annulus they bound) or at least one deepest disk pair (with no component of D' inside either disk). Since the Pinkall invariant is 0 on any component of D', the image of such an annulus is a C^0-embedded torus in $\tilde{i}(\mathbb{P}^2)$ and the image of such a disk pair is a C^0-imbedded sphere in $\tilde{i}(\mathbb{P}^2)$. In both cases these non-trivial 2-cycles in $H_2(\tilde{i}(\mathbb{P}^2), \mathbb{Z}_2)$ can be removed by a simple surgery modification $\tilde{i}' : \mathbb{P}^2 \to \mathbb{S}^3$ which changes $\tilde{i}$ only on a neighborhood of this deepest annular or disk pair. This surgery reduces the number of components in D'.

Theorem 5.2. *Let $\tilde{i} : \mathbb{P}^2 \to \mathbb{S}^3$ be a generic immersion with one triple point and $(1 + k)$ components in the self-intersection set $\tilde{\mathcal{S}}_1 \subseteq \tilde{\mathcal{S}} \subseteq \mathbb{S}^3$. There exists a sequence of spherical or toral surgery modifications $\tilde{i}_1, \tilde{i}_2, \ldots, \tilde{i}_k$ as described above which terminate with $\tilde{i}_k \equiv i_{b^\pm}$ or $i_{g^\pm}$. Each subsequent modification reduces the first and second $\mathbb{Z}_2$-Betti numbers by 1. The $\mathbb{Z}_2$-Betti numbers of $\tilde{i}(\mathbb{P}^2) = \tilde{\mathcal{S}}$ are given by $\beta_1 = k$, $\beta_2 = k + 1$.*

Proof. Each surgery modification removes exactly one non-trivial 2-cycle in $\mathcal{S}$ (a sphere or a torus). By the Boy–Izumiya–Marar formula [11], $\chi(\tilde{\mathcal{S}}) = \chi(\mathbb{P}^2) + (\#\text{ triple points}) = 2$, hence each surgery must also remove a non-trivial 1-cycle. By Theorem 4.3, after k of these surgeries, we have $\tilde{i}_k \equiv i_{b^\pm}$ or $i_{g^\pm}$. We need only show the first and second Betti numbers for both $i_{b^\pm}$ and $i_{g^\pm}$ are 0 and 1 respectively. To see this, observe that every 2-cycle must correspond to a union of image disks in $\mathbb{P}^2 - D$ which arise from the immersion-adapted decomposition. Direct inspection of the three-critical-point models in Section 1 reveals that removing any number of these disks creates a $\mathbb{Z}_2$-boundary in the 2-chain, hence the second homology of the images has exactly one generator. □

5.3. Almost tight ambient isotopy classes

The models of Section 1 reveal that the complements of each of the images of $i_{b^\pm}$ and $i_{g^\pm}$ has two components. Choosing a point at infinity in each component respectively yields two distinct ambient isotopy classes of immersions into $\mathbb{R}^3$ for each of the four models in $\mathbb{S}^3$. With simple modifications of the level curves in Section 1, each of the eight classes of immersions into $\mathbb{R}^3$ can be represented by an immersion with exactly three non-degenerate critical points. An example of such a level curve modification can be found in [12] where Kuiper sought restrictions on tight mappings.

Recall that an immersion of a compact surface into Euclidean 3-space $i : M \to \mathbb{R}^3$ is ***tight*** if its total curvature $\tau(i) = \frac{1}{2\pi} \int_M |K| \, dA$ equals $\beta(M)$, the sum of the $\mathbb{Z}_2$-Betti numbers of M. Following Kuiper [4,15], we say an ambient isotopy class

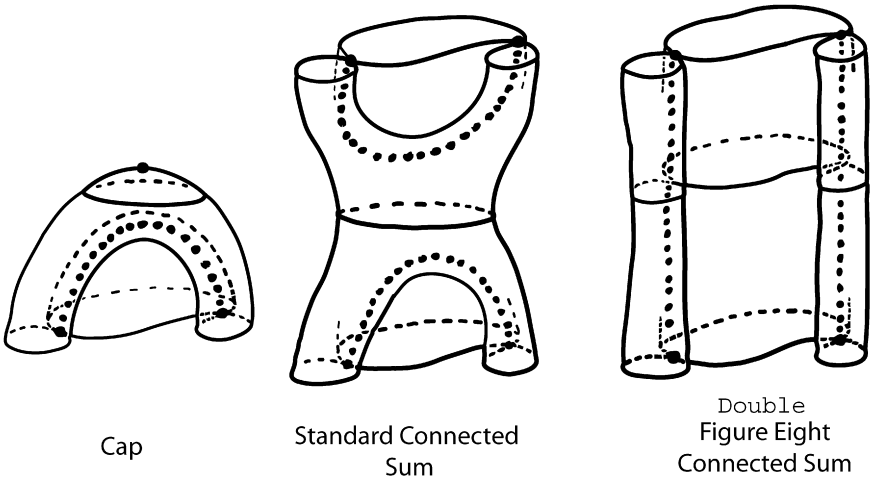

Fig. 5.1.

of immersions in $\mathbb{R}^3$ is *almost tight* if, for all $\varepsilon > 0$, there exists a representative immersion whose total curvature lies within ε of $\beta(M)$ (i.e., $\beta(M)$ is the *inf* of total curvature over this set of immersions). Now if $i : M \to \mathbb{R}^3$ is an immersion which has a non-degenerate height function $h : \mathbb{R}^3 \to \mathbb{R}$ with exactly one max and one min, then

$$i_\varepsilon = i + \frac{1}{\varepsilon}\big(\mathit{Grad}(h)\big), \quad \varepsilon > 0,$$

has $\lim_{\varepsilon\to 0} \tau(i_\varepsilon) = \beta(M)$. Hence the existence of the above eight distinct immersions of $\mathbb{P}^2$ (each with $\beta(\mathbb{P}^2) = 3$ non-degenerate critical points) implies that the eight associated ambient isotopy classes are each almost tight. Moreover, given a positive integer n, we can construct generic immersions of the n-fold connected sum $i : n\mathbb{P} \to \mathbb{R}^3 \subseteq \mathbb{S}^2$ using the two types of ambient connected sum in Fig. 5.1. We can stack these connected sums in the direction of increasing height so that the resulting immersion will have $\beta(n\mathbb{P}) = 2 + n$ non-degenerate critical points. Thus the various combinations of the two types of connected sum using $i_{b^\pm}$ and $i_{g^\pm}$ produce a large collection of distinct, almost tight, ambient isotopy classes of immersed non-orientable surfaces with n triple points.

Acknowledgements

We are indebted to A. Mellnik for his innovative CAD "cut-and-paste" constructions and renderings (see Figs. 3.10 and 3.11). It was his discovery of $\mathbb{Z}_2$-symmetric models which inspired Corollary 5.1. We also thank the referee for his helpful comments and suggestions.

References

[1] F. Apéry, The boy surface, Adv. Math. 61 (1986) 185–266.
[2] F. Apéry, Models of the Real Projective Plane: Computer Graphics of Steiner and Boy Surfaces, Vieweg, Braunschweig, Germany, 1987.
[3] T. Banchoff, Triple points and singularities of projections of smoothly immersed surfaces, Proc. AMS 46 (3) (1974) 407–413.
[4] T. Banchoff, W. Kühnel, Tight submanifolds, smooth and polyhedral, in: T.E. Cecil, S.-s. Chern (Eds.), Tight and Taut Submanifolds, Cambridge Univ. Press, 1997, pp. 51–118.
[5] W. Boy, Über die Curvatura integra und die Topologie geschlossener Flächen, Math. Ann. 57 (1903) 151–184.
[6] J.S. Carter, How Surfaces Intersect in Space, World Scientific, 1993.
[7] J.S. Carter, M. Saito, Knotted Surfaces and Their Diagrams, Mathematical Surveys and Monographs, vol. 55, AMS, 1998.
[8] P.J. Eccles, Multiple points of codimension one immersion, in: U. Koshorke (Ed.), Top. Sym. Siegen, in: Lecture Notes in Math., vol. 788, Springer-Verlag, Berlin, New York, 1979, pp. 23–38.
[9] G. Francis, A Topological Picturebook, Springer Verlag, 2007.
[10] H.R. Farran, Pinto, M. do Rosario, S.A. Robertson, Symmetric models of the real projective plane, Beiträge zur Algebra und Geometrie (Contributions to Algebra and Geometry) 40 (1) (1999) 195–202.
[11] S. Izumiya, W.L. Marar, The Euler characteristic of a generic wave front in a 3-manifold, Proceedings A.M.S. 118 (1993) 1347–1350.
[12] N. Kuiper, Stable surfaces in Euclidean three space, Math. Scand. 36 (1975) 83–96.
[13] B. Morin, J.-P. Petit, Le retournement de la sphere, C. R. Acad. Sci. Paris Ser. A–B 287 (11) (1978) A791–A794.
[14] U. Pinkall, Regular homotopy classes of immersed surfaces, Topology 24 (4) (1984) 421–434.
[15] U. Pinkall, Tight surfaces and regular homotopy, Topology 25 (4) (1985) 475–481.
[16] D. Rolfsen, Knots and Links, Mathematics Lecture Series, vol. 7, Publish or Perish, Inc., 1976.
[17] D. Roseman, Reidemeister-type moves for surfaces in four space, in: V.F.R. Jones, J. Kania-Bafrtoszynska, V. Turaev, J.H. Przytycki, P. Traczyk (Eds.), Knot Theory, in: Banach Center Publications, vol. 42, 1998.
[18] H. Schubert, Knotten und Vollringe, Acta Math. 90 (1953) 131–286.